Published by
NIGERIAN SOCIETY OF PHYSICAL SCIENCES
Available online @ https://journal.nsps.org.ng/index.php/jnsps

J. Nig. Soc. Phys. Sci. 4 (2022) 9–15

Journal of the Nigerian Society of Physical Sciences

Investigations of the Elastic Moduli of Er_2O_3NPs NPs Doped $TeO_2 - B_2O_3 - SiO_2$ Glasses using Theoretical Models

U. S. Aliyu[a,*], I. G. Geidam[b], M. S. Otto[a], M. Hussaini[c]

[a] *Department of Physics, Faculty of Science, Federal University Lafia, Nasarawa Sate, Nigeria*
[b] *Department of Physics, Faculty of Sciences, Yobe State University Damaturu, Nigeria*
[c] *Department of Physics, Faculty of Sciences, Umar Suleiman College of Education Gashua, Yobe State, Nigeria*

Abstract

Elastic moduli of $\{[(TeO_2)_{0.7}\ (B_2O_3)_{0.3}]_{0.8}\ (SiO_2)_{0.2}\}_{1-y}\ (Er_2O_3\ NPs)_y$ glasses with y = 0.01, 0.02, 0.03, 0.04, 0.05 were studied in this work using the theoretical elastic models. The Makishima & Mackenzie, Rocherulle and bond compression models were employed for the study. In the Makishima and Mackenzie model, the packing density was calculated from the bulk glass molar weight and the bulk glass density whereas in Rocherulle model it is determined as the individual oxides. Young, shear and bulk moduli as well as the Poisson ratio were calculated for the glasses in the Makishima and Rocherulle models, while longitudinal, was calculated in addition to young, bulk and shear moduli using the bond compression model. Bond per unit volume number (n_b), bulk modulus, bulk modulus ratio (K_{bc}/K_e), atomic ring size (ℓ) and stretching force constantwere also calculated and presented. The values of the Young, bulk and shear moduli obtained from Makishima model increased from 52.854 to 55.335 GPa, 35.754 to 39.862GPa and 21.080 to 21.809GPa respectively with Er_2O_3NPs composition increase from 1% to 5%..The Rocherulle model presented increasing values for Young, bulk and shear moduli as 56.910 to 58.432GPa, 41.452 to 44.450 GPa and 22.385 to 22.809 GPa respectively with Er_2O_3NPs composition increase from 1% to 5%. The bond compression model presented much higher values of the elastic moduli compared to the experimentally obtained values and showed an increasing trend as the Er_2O_3NPs concentration increases. In the glass network, the atomic ring size value decreased from 0.5698 to 0.5091 nm indicating an increase in the close packing of atoms. Based on the elastic moduli values presented by all the models, Makishima and Mackenzie model presented a more reliable data and hence represents the best model for the studied glass system.

DOI:10.46481/jnsps.2022.222

Keywords: Erbium oxide, Tellurite Glass, Elastic Moduli, Poisson Ratio, Theoretical Models

Article History :
Received: 05 May 2021
Received in revised form: 04 December 2021
Accepted for publication: 05 December 2021
Published: 28 February 2022

Communicated by: B. J. Falaye

1. Introduction

Tellurite based glasses doped with rare earth ions have been used in amorphous silicon solar cells for the improvement of the cell efficiency [1]. These glasses are developed widely in various optical applications in glass sensors, optoelectronics, fibre optics and light emitting diode (LED) [2, 3, 4, 5]. In most cases glasses requiring mechanical strength for special applications are fabricated in combination with SiO_2as silica combination is known to provide thermal stability, mechanical strength and chemical stability [6, 7, 8, 9]. Silica incorporation in glasses improves their optical transparency in both lasing and excitation wavelengths [10]. B_2O_3 is considered an excellent raw material in combination with other TeO_2 based glasses for quality

*Corresponding author tel. no: +2348039364898
Email address: usaltilde@yahoo.com (U. S. Aliyu)

improvement in terms of hardness, optical transparency, easy glass fabrication (as it lowers the glass's melting temperature) and rare earth ion solubility [11].

Various researchers in the area of glass science, technology and engineering have been engaged in the study of different glass properties for applications in the areas of communications, optical, laser and other [12, 13, 14]. Glass's application in any technology is affected by either its mechanical strength, optical behaviours, elastic properties, thermal stability or chemical stability [15, 16].Because of mechanical strength importance in optical disc, optical fibres medical and dental implants, electronic displays and radiation shielding applications, SiO_2 are used as substrates to provide such mechanical strengths [17, 18, 19].

Elastic moduli of glasses of different compositions have been studied by various researchers over the years. Makishima and Mackenzie developed a model for the calculation of the elastic moduli of glasses theoretically, in consideration to its importance in the manufacture of strong optical fibres [20, 21]. Rocherulle et al. [22] proposed a model that improved the Makishima and Mackenzie model through the extension of the dissociation energy and packing factors. The bond compression model is based on the consideration of the oxides' atomic geometry which include their coordination number as well bond length [23].

In this work, the elastic moduli of the Er_2O_3 doped $TeO_2 - B_2O_3 - SiO_2$ glasses were determined using Mackishima and Mackenzie, Rocherulle and bond compression models. The study of the elastic moduli is important for the definition of its applicability in optical fibre, laser and other optoelectronic applications. The objectives of the study are as follows;

1. To determine the elastic moduli of the glasses under study using theoretical models.
2. To compare the values of the elastic moduli obtained from each model with the others.

This work is important considering the importance of the elastic moduli to the application in different areas of technology and the fact that there is no such work carried out on the studied glasses composition.

2. Theoretical Models

This section presents the four theoretical models adopted in this work for the study of the elastic properties of the Er_2O_3 and Er_2O_3 NPs doped rice husk silicate borotellurite glass systems. The models used include the Makishima-Mackenzie model, Rocherulle model, bond compression model and the ring deformation model.

2.1. Makishima and Mackenzie model

The Makishima and Mackenzie model proposed a theoretical approach to determine the elastic moduli of oxide glasses with consideration to to the chemical composition (x_i) of the constituting oxide, individual oxides' packing densities (V_i), and their corresponding dissociation energies (G_i) [24]. The glass Young modulus is expressed in terms of the packing density (V_t), and the dissociation energy (G_t) as;

$$E_m = 2V_t \sum_i G_i x_i = 2V_t G_t \tag{1}$$

From the oxides' packing density, $V_t$can be determined as by

$$V_t = \left(\frac{\rho}{M}\right) \sum_i V_i x_i \tag{2}$$

where M = glass molecular weight, ρ = glass density, x_i $=i_{th}$component's molar fraction (i), and V_i is calculated for an oxide (A_x O_y) as:

$$V_i = N_A\,(4\pi/3)\left(xR_A^3 + yR_O^3\right), \tag{3}$$

where R_O and R_A respectively represent the ionic radii of oxygen and cation respectively [23]. According to Makishima and Mackenzie, bulk modulus (K_m), Shear modulus (G_m)and Poisson ratio (σ_m) for oxide glasses on any component are calculated as follows:

$$K_m = 1.2V_t E \tag{4}$$

$$G_m = (3EK/9K - E) \tag{5}$$

$$\sigma_m = (E/2G_m - 1) \tag{6}$$

2.2. Rocherulle Model

A modified expressions of the Makishima and and Mackenzie model was proposed by Rocherulle at al. (1989) [22]. The packing density, V_i in the Makishima-Mackenzie model is replaced with C_i which is expressed as follows:

$$C_i = N_A\,(4\pi\rho/3M)\left(xR_A^3 + yR_O^3\right) \tag{7}$$

For glasses of polycomponent nature, the C_t factor is therefore expressed as follows:

$$C_t = \sum_i C_i x_i \tag{8}$$

$$C_i = \sum_i \frac{\rho_i}{M_i} V_i x_i \tag{9}$$

The Young Modulus (E_r), bulk modulus (K_r), shear modulus (G_r) and the Poisson ratio are calculated as in equations (1), (4), (5), and (6) respectively. The basic difference between the two models is that the Makishima and Mackenzie model take into consideration the bulk density and molecular weight of the glass, while the Rocherulle model considers the individual oxides' density and molecular weights [22].

2.3. Bond Compression and Ring Deformation Models

The theoretical model of bond compression takes into consideration the atomic networking in a material and the bond stretching force constants between them to theoretically estimate the elastic characteristics of the material [25]. For single oxide glass systems, the bulk modulus is obtained as;

$$K_{bc}=\frac{n_b\overline{F}r^2}{9} \tag{10}$$

The expression for a multicomponent oxide glasses is given as:

$$K_{bc} = (\rho N_A/9M)\sum_i (xn_f\overline{F}r^2)_i, \tag{11}$$

where $\overline{F}$ = the average stretching force constant, and n_b= the bond number per unit volume and r is the cation-anion bond length.

The bond number per unit volume is calculated as:

$$n_b = \left(n_f\rho N_A/M\right) \tag{12}$$

n_f is the number of bonds per unit glass formula, ρ is the glass density,N_A is Avogadro's number and M is the glass molecular weight [26]. The stretching force constant (f) is deduced for multi-component glass using the expression as reported by [27] as:

$$\overline{F}=\frac{\sum_i\left(xn_f f\right)_i}{\sum_i\left(xn_f\right)_i} \tag{13}$$

The calculations of Poisson's ratio (σ_{bc}) and the corresponding average cross link density ($\overline{n}_c$) of the glasses are deduced as in equations (13) and (14) respectively.

$$\sigma_{bc} = 0.28(\overline{n}_c)^{-0.25} \tag{14}$$

$$\overline{n}_c = \frac{1}{\eta}\sum_i (xn_cN_c)_i, \tag{15}$$

where n_c= oxide (i) cross-link number per cation and N_c= cation number per unit glass formula.

The total number of cations per unit glass formula for a multicomponent glass system (η) is obtained as:

$$\eta = \sum_i (xN_c)_i \tag{16}$$

K_{bc} and σ_{bc} are used to calculate the Young, shear and longitudinal moduli. The ring deformation model theoretically estimates the atomic ring size in the glass network structure. The model uses the experimental bulk modulus (K_e) values and the bending force constant (F_b) values to estimate the atomic ring size [28]. In the approximation process, the average stretching force constant is used in place of F_b.

The following formula is used in the determination of the atomic ring size:

$$K_e = 0.0106F_b(l)^{-3.84} \tag{17}$$

The value l represents the atomic ring size and is defined as the diameter of the external ring. The ring perimeter can be determined using l as bond number x bond length divide by π [29].

3. Results and Discussions

4. Makashima Model

Using the Makishima and Mackenzie model, the results of the theoretical elastic properties data obtained is presented in this section.

Figure 1 illustrates the packing density and dissociation energy variation of the $\{[(TeO_2)_{0.7}\ (B_2O_3)_{0.3}]_{0.8}\ (SiO_2)_{0.2}\}_{1-y}$ $(Er_2O_3\ NPs)_y$ glass system with increasing concentration of Er_2O_3NPs. The packing density value increased from 0.5637 to 0.6003 cm^{-3}. The value increases maybe associated to the increment in the density of the material. This increment is connected to increase in the material compactness and rigidity. It can also be said to be due to increase in the conversion of TeO_3 to TeO_4 structural form [30].

The dissociation energy decreased from 46.878 to 46.088 kJ/cm^3 with the increased Er_2O_3 concentration from 1% to 5%. The decrease in the value maybe due to the introduction of more low dissociation energy Er_2O_3 into the system. It may also relate to the observed increase in the molar volume of the glasses [31].

Figure 2 and Table 1 presents the elastic moduli of the glass system of $\{[(TeO_2)_{0.7}\ (B_2O_3)_{0.3}]_{0.8}\ (SiO_2)_{0.2}\}_{1-y}$ $(Er_2O_3\ NPs)_y$ composition. The Young, bulk and shear moduli increased from 52.8537 to 55.3347 GPa, 35.7544 to 39.8619 GPa and 21.0804 to 21.8087 GPa respectively. The increase in the elastic moduli increase with increase in the Er_2O_3 concentration may be due to increase in material compactness associated with increase in the TeO_4 units' concentration. The elastic moduli increase is generally associated with rigidity increase [15, 32].

The Poisson ratio value for the $\{[(TeO_2)_{0.7}\ (B_2O_3)_{0.3}]_{0.8}$ $(SiO_2)_{0.2}\}_{1-y}$ $(Er_2O_3\ NPs)_y$ presented in Table 1 increased from 0.2536 to 0.2686 with the increase in the Er_2O_3 concentration from 1% to 5%. The Poisson ratio increases normally with increase in the crosslink density of a material [33]. According Makishima and Mackenzie, Poisson ratio of a silicate glass should be around 0.25 when the work done after glass deformation involves the compression or stretching of the Si-O-Si links [21].

5. Rocherulle's Model

Table 2 presents the packing density, elastic moduli, and the Poisson ratio values for the glass system of $\{[(TeO_2)_{0.7}$ $(B_2O_3)_{0.3}]_{0.8}\ (SiO_2)_{0.2}\}_{1-y}\ (Er_2O_3\ NPs)_y$composition. The packing density values increased from 0.6008 to 0.6094 when the Er_2O_3 concentration was increased from 1% to 5%. The increase in the packing density might be due to the decrease in the interatomic spaces resulting from the formation of more bridging oxygens (BOs) with the formation of more TeO_4 structural units in the glass network [34]. This can also be due to the formation of more BO_3 units and decreasing concentration of BO_2O nature containing one (1) non-bridging oxygen (NBO) and two (2) bridging oxygen atoms attacked to the boron atom [35].

Table 1: Packing Density (V_t), Dissociation Energy (G_t), Elastic Moduli (E_m, K_m and G_m) and Poisson Ratio (σ_m) for glass system of $\{[(TeO_2)_{0.7}\ (B_2O_3)_{0.3}]_{0.8}\ (SiO_2)_{0.2}\}_{1-y}\ (Er_2O_3\ NPs)_y$composition.

y (mol)	V_t $\left(cm^3\ mol^{-1}\right)$	G_t (KJ/cm^3)	E_m (GPa)	K_m (GPa)	G_m (GPa)	σ_m
0.01	0.5637	46.8784	52.8538	35.7544	21.0804	0.2536
0.02	0.5710	46.6809	53.3064	36.5233	21.2081	0.2567
0.03	0.5755	46.4833	53.4977	36.9424	21.2521	0.2586
0.04	0.5879	46.2857	54.4262	38.3990	21.5333	0.2638
0.05	0.6003	46.0882	55.3347	39.8619	21.8087	0.2686

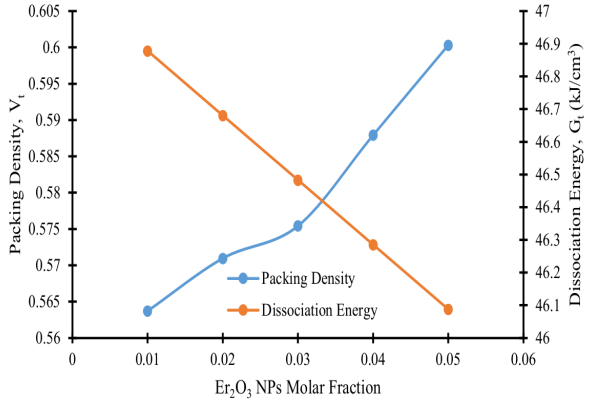

Figure 1: Packing density and dissociation energy variation with the molar fraction of Er_2O_3NPs in $\{[(TeO_2)_{0.7}\ (B_2O_3)_{0.3}]_{0.8}\ (SiO_2)_{0.2}\}_{1-y}\ (Er_2O_3\ NPs)_y$ glass system

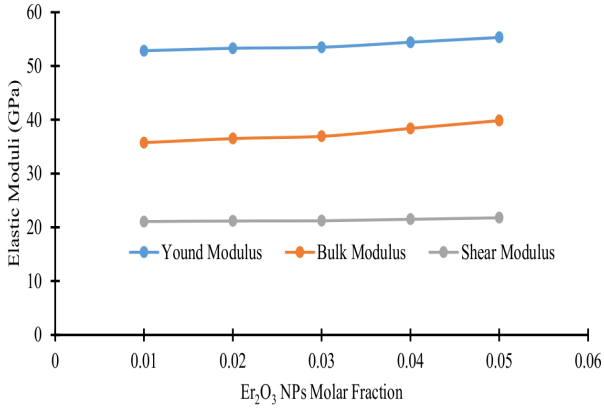

Figure 2: The variation of the elastic moduli with molar fraction of Er_2O_3 in $\{[(TeO_2)_{0.7}\ (B_2O_3)_{0.3}]_{0.8}\ (SiO_2)_{0.2}\}_{1-y}\ (Er_2O_3\ NPs)_y$ glass system

The Young and shear moduli increased from 56.9097 to 58.4324 GPa and 22.3445 to 22.8090 GPa, respectively with an increase in the Er_2O_3 molar fraction from 0.01 to 0.05. The decrease in the values may be associated with decrease in the dissociation energy which overrides the observed increase in the packing density. The bulk modulus was found to have increased from 41.4525 to 44.4498GPa. The bulk modulus increase might be due to the increase observed in the packing density of the glasses. The bulk modulus dependence to the packing density is more than its dependence on the dissociation

Table 2: Packing density (C_t), elastic moduli (E_R, K_R, and G_R), Poisson ratio (σ_R) for glass systemof $\{[(TeO_2)_{0.7}\ (B_2O_3)_{0.3}]_{0.8}\ (SiO_2)_{0.2}\}_{1-y}\ (Er_2O_3\ NPs)_y$composition.

y (mol)	C_t $\left(cm^3\ mol^{-1}\right)$	E_R (GPa)	K_R (GPa)	G_R (GPa)	σ_R
0.01	0.6070	56.910	41.452	22.385	0.2712
0.02	0.6137	57.298	42.198	22.493	0.2737
0.03	0.6205	57.682	42.947	22.600	0.2762
0.04	0.6272	58.060	43.697	22.705	0.2786
0.05	0.6339	58.432	44.450	22.809	0.2809

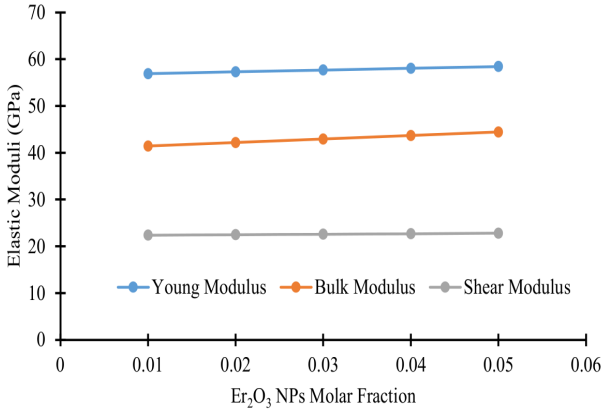

Figure 3: Elastic moduli variation with molar fraction of Er_2O_3NPs for glass systemof $\{[(TeO_2)_{0.7}\ (B_2O_3)_{0.3}]_{0.8}\ (SiO_2)_{0.2}\}_{1-y}\ (Er_2O_3\ NPs)_y$ composition.

energy [22]. This leads to the overriding effect of the packing density on the bulk modulus value than the dissociation energyon the bulk modulus value [36].

The Poisson ratio value for the glass system of $\{[(TeO_2)_{0.7}\ (B_2O_3)_{0.3}]_{0.8}\ (SiO_2)_{0.2}\}_{1-y}\ (Er_2O_3\ NPs)_y$composition as shown in Table 2 increased from 0.2712 to 0.2809 as the Er_2O_3concentration increased from 1% to 5%. The Poisson ratio is a rigidity dependent parameter, as such increase in the Poisson ratio maybe due to an increase in the rigidity of the glasses. This is due to the closure of the interstices between atoms in the glass network This allows large structural relaxation with the introduction of the sound waves, which makes the lateral strain to grow larger compared to the longitudinal strain [31]. The increase can also be attributed to the decrease in the iconicity caused by the introduction of more polar Er^{3+}

ions in the network [37].

6. Bond Compression Model and Ring Deformation Model

The results of the elastic moduli and the Poisson ratio calculated using the bond compression model for the$\{[(TeO_2)_{0.7}(B_2O_3)_{0.3}]_{0.8}(SiO_2)_{0.2}\}_{1-y}(Er_2O_3\ NPs)_y$glassesare presented in this section. Also discussed in this section is the ring deformation model results for the glass system of $\{[(TeO_2)_{0.7}(B_2O_3)_{0.3}]_{0.8}(SiO_2)_{0.2}\}_{1-y}(Er_2O_3\ NPs)_y$ composition.

Figure 4 and Table 3 presents the variation of the bond per unit volume number and the average stretching force constant with molar fraction of Er_2O_3 composition for the glass system of $\{[(TeO_2)_{0.7}(B_2O_3)_{0.3}]_{0.8}(SiO_2)_{0.2}\}_{1-y}(Er_2O_3\ NPs)_y$ composition. The bond number per unit volume increased, decreased and then increased with the increase in the Er_2O_3 concentration. The increase in the value might be due to the increase in the number of TeO_4 and BO_3 structures with decreasing number of TeO_3 and BO_2O structures, indicating an increase in the number of bridging oxygen [31]. It can also be attributed with observed increase in cross-link density [36] as shown in Table 3. The decrease in the value maybe also associated with the increase in the glasses' molar volume resulting from increased interstitial spacing between constituting glass atoms [34].

The value of the average stretching force constant for the studied glasses decreased from 362.5248 to 349.8995 Nm^{-1} as the Er_2O_3 NPs concentration increased from 1% to 5%. The decrease in the first order average stretching force constant might be associated with the substitution of oxides of higher stretching force constant; SiO_2 [25], B_2O_3 [38] and TeO_2 [39] with Er_2O_3 [14, 15] having much lower stretching force constant value.

The elastic moduli for glass system of $\{[(TeO_2)_{0.7}(B_2O_3)_{0.3}]_{0.8}(SiO_2)_{0.2}\}_{1-y}(Er_2O_3\ NPs)_y$ composition is presented in Figure 5 and Table 4. The values of the bulk, shear, longitudinal and Young moduli ranged from 79.56544 to 81.35993 GPa, 53.76034 to 55.97828 GPa, 151.2532 to 155.9976GPa and 131.636 to 1236.6052GPa respectively with increase in the Er_2O_3 concentration from 1% to 5%. Generally, Young modulus is related to the bond stretching force constant whereas the shear modulus is related to the bond bending force constants of the constituting oxides of a glass [37].The decrease in the values of the moduli maybe due the introduction of Er_2O_3 with larger cation-anion length (r= 0.225 nm) compared to the substituted TeO_2 (with r = 199 nm), B_2O_3 (r=0.138 nm) and SiO_2 (r= 161) [23, 25, 40]. The decrease reflects the dependence of the elastic moduli on the average stretching force constant which decrease due the introduction of more Er_2O_3 lower stretching force constant [41].

Figure 6 presents the variation of the atomic ring size of the glass systemof $\{[(TeO_2)_{0.7}(B_2O_3)_{0.3}]_{0.8}(SiO_2)_{0.2}\}_{1-y}(Er_2O_3\ NPs)_y$composition with Er_2O_3 molar fraction. The atomic ring size value decreased from 0.5996 to 0.5786 nm when the Er_2O_3 concentration was increased from 1% to 5%. The decreased in the value maybe attributed to the increase in density, crosslink density and rigidity of the glasses [37]. This implies the close packing of the material in the glass network [42].

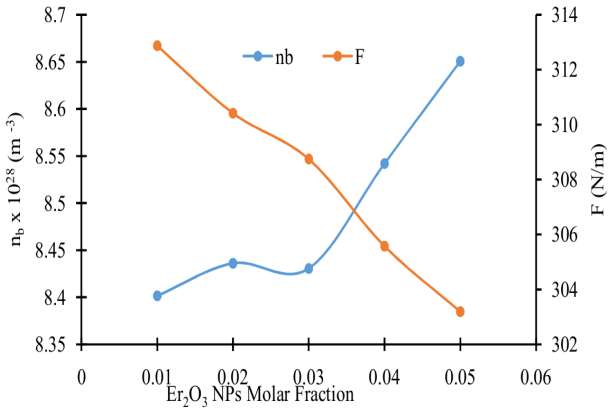

Figure 4: Bond per unit volume and stretching force constant variation with molar fraction of Er_2O_3NPs for glass system of $\{[(TeO_2)_{0.7}(B_2O_3)_{0.3}]_{0.8}(SiO_2)_{0.2}\}_{1-y}(Er_2O_3\ NPs)_y$composition.

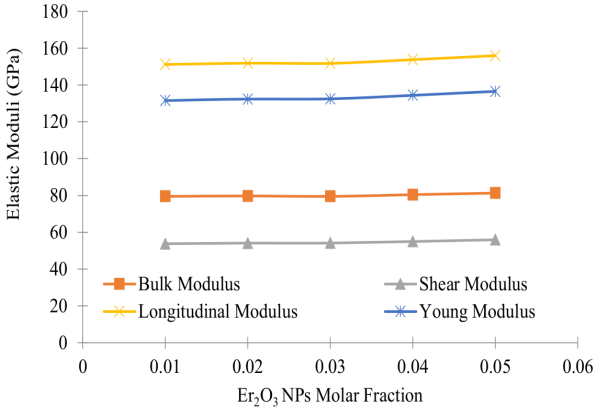

Figure 5: Elastic moduli variation with molar fraction of Er_2O_3 for glass system of $\{[(TeO_2)_{0.7}(B_2O_3)_{0.3}]_{0.8}(SiO_2)_{0.2}\}_{1-y}(Er_2O_3\ NPs)_y$ composition.

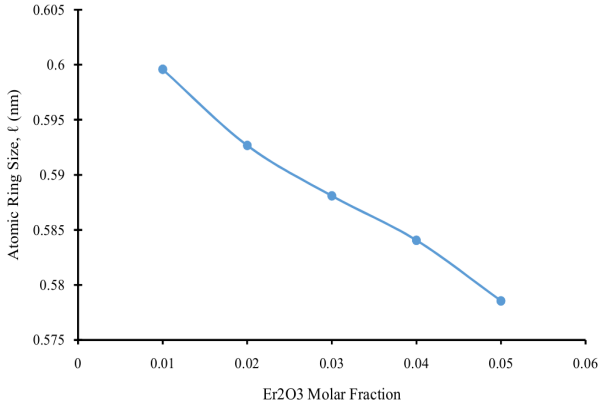

Figure 6: Atomic ring size variation with molar fraction of Er_2O_3 for glass system of $\{[(TeO_2)_{0.7}(B_2O_3)_{0.3}]_{0.8}(SiO_2)_{0.2}\}_{1-y}(Er_2O_3\ NPs)_y$ composition

Table 5 presents the elastic moduli (Young, bulk and shear moduli) obtained from experiment and theoretical models of Makishima & Mackenzie, Rocherulle and Bond compression. The data from Makishima & Mackenzie model presented a much closer elastic moduli values to the experimental values compare to the Rocherulle and bond compression models. The

Table 3: Bond per unit volume number (n_b), bulk modulus, bulk modulus ratio (K_{bc}/K_e), atomic ring size (ℓ) and stretching force constant (F) for $\{[(TeO_2)_{0.7}(B_2O_3)_{0.3}]_{0.8}(SiO_2)_{0.2}\}_{1-y}(Er_2O_3\ NPs)_y$ glass system.

y	n_b ($\times10^{28}$ m^{-3})	K_{bc} (GPa)	K_e (GPa)	K_{bc}/K_e	l (nm)	F (N/m)	n_c
0.01	8.4014	79.5728	30.6560	2.5957	0.5828	362.525	2.4289
0.02	8.4360	79.7584	31.1124	2.5636	0.5792	359.322	2.4704
0.03	8.4304	79.5654	33.3348	2.3869	0.5680	357.029	2.5112
0.04	8.5419	80.4765	41.1798	1.9543	0.5360	353.009	2.5516
0.05	8.6507	81.3599	43.1171	1.8870	0.5284	349.900	2.6161

Table 4: Elastic moduli and Poisson ratio for glass system of $\{[(TeO_2)_{0.7}(B_2O_3)_{0.3}]_{0.8}(SiO_2)_{0.2}\}_{1-y}(Er_2O_3\ NPs)_y$ composition.

y	K_{bc} (GPa)	G_{bc}(GPa)	L_{bc}(GPa)	E_{bc}(GPa)	$\boldsymbol{\sigma}_{bc}$
0.01	79.5738	53.7603	151.253	131.636	0.22429
0.02	79.7584	54.1123	151.908	132.396	0.22334
0.03	79.5654	54.2003	151.833	132.512	0.22243
0.04	80.4765	55.0357	153.858	134.457	0.22154
0.05	81.3599	55.9783	155.998	136.605	0.22016

Table 5: Comparative presentation of Bulk, Young and Shear moduli obtained from non-destructive ultrasonic spectroscopic analysis (experimental) and Makishima & Mackenzie, Rocherulle and Bond compression models

y	Bulk Modulus				Young Modulus				Shear Modulus			
	K_e	K_m	K_r	K_{bc}	E_e	E_m	E_r	E_{bc}	G_e	G_m	G_r	G_{bc}
0.01	30.656	35.754	41.452	79.573	31.801	52.854	56.910	131.64	20.546	21.080	22.385	53.760
0.02	31.112	36.523	42.198	79.758	33.951	53.306	57.298	132.40	21.685	21.208	22.493	54.112
0.03	33.335	36.942	42.947	79.565	34.770	53.498	57.682	132.51	22.436	21.252	22.600	54.200
0.04	41.180	38.399	43.697	80.477	35.412	54.426	58.060	134.46	23.841	21.533	22.705	55.036
0.05	43.117	39.862	44.450	81.360	37.720	55.335	58.432	136.61	25.302	21.809	22.809	55.978

values of the elastic moduli from the elastic models showed an increasing trend just as obtained from the experimental data but demonstrating comparatively very high values from the bond compression model. Data obtained from the Rocherulle model showed a very much closer relation to the data obtained from the experimental assessment compared to the bond compression model. The increase in the elastic moduli is generally associated with increased rigidity and network connectivity [43, 44].

7. Conclusions

Makishima and Mackenzie, Rocherulle and bond compression models were used in this work for the theoretical determination of the elastic moduli of Er^{3+} ions doped silica borotellurite glass system with empirical formula $\{[(TeO_2)_{0.7}(B_2O_3)_{0.3}]_{0.8}(SiO_2)_{0.2}\}_{1-y}(Er_2O_3\ NPs)_y$ with y = 0.01, 0.02, 0.03, 0.04, 0.05. The elastic moduli (Young, shear and bulk) increased with increasing concentration of Er_2O_3 in the Makishima and Mackenzie model. The values of the elastic moduli calculated presented a decreasing value of Young and shear elastic moduli with increasing pattern of the corresponding bulk modulus value as the Er_2O_3 concentration was increased. The bond compression model presented rather much higher values of the elastic moduli compared to the other two models with an increasing value variation against the Er_2O_3 molar concentration. This might be due to the fact that, unlike the Makishima & Mackenzie and Rocherulle models which commonly considers densities and dissociation energies, the bond compression model considers the bond strength and numbers. Among the three models considered in this work, the Makishima and Mackenzie model presented a more reasonable values of the elastic moduli and thus can be regarded as the best model for the studied glass system.

References

[1] N. Elkhoshkhany, R. Abbas, M. S. Gaafar, and R. El-Mallawany, "Elastic properties of quaternary TeO2-ZnO-Nb2O5-Gd2O3 glasses", Ceram. Int. **41** (2015) 9862 doi: 10.1016/j.ceramint.2015.04.060.

[2] M. N. Azlan, M. K. Halimah, A. B. Suriani, Y. Azlina, S. A. Umar, and R. El-mallawany, "Upconversion properties of erbium nanoparticles doped tellurite glasses for high efficient laser glass", Opt. Commun. **448** (2019) 82. doi: 10.1016/j.optcom.2019.05.022.

[3] S. H. Alazoumi et al., "Optical properties of zinc lead tellurite glasses", Results Phys. **9** (2018) 1371. doi: 10.1016/j.rinp.2018.04.041.

[4] H. R. Shaari et al., "Investigation of Structural and Optical Properties of Graphene Oxide - Coated Neodymium Nanoparticles Doped Zinc -

Tellurite Glass for Glass Fiber", J. Inorg. Organomet. Polym. Mater. **31** (2021) 1, doi: 10.1007/s10904-021-02061-7.

[5] S. A. Umar et al., "Oxide ion / electronic polarizability , optical basicity and linear dielectric susceptibility of TeO2 – B2O3 – SiO2 glasses", Ceram. Int. **47** (2021) 21668, doi: 10.1016/j.ceramint.2021.04.180.

[6] N. Berwal, S. Dhankhar, P. Sharma, R. S. Kundu, R. Punia, and N. Kishore, "Physical , structural and optical characterization of silicate modi fi ed bismuth-borate-tellurite glasses", J. Mol. Struct. **1127** (2017) 636, doi: 10.1016/j.molstruc.2016.08.033.

[7] I. G. Geidam et al., "Thermo-physical and elastic properties of Bi2O3 doped silica borotellurite glasses", Optik (Stuttg). **248** (2021) 12, doi: 10.1016/j.ijleo.2021.168201.

[8] M. K. Halimah, A. A. Awshah, A. M. Hamza, S. A. Umar, K. T. Chan, and S. H. Alazoumi, "Effect of neodymium nanoparticles on optical properties of zinc tellurite glass system", J. Mater. Sci. Mater. Electron. **31** (2020) 3785, doi: 10.1007/s10854-020-02907-9.

[9] M. K. Halimah et al., "Study of rice husk silicate effects on the elastic, physical and structural properties of borotellurite glasses", Mater. Chem. Phys. **238** (2019) 121891, doi: 10.1016/j.matchemphys.2019.121891.

[10] S. A. Umar, M. K. Halimah, A. M. Hamza, and A. A. Abdulbaset, "The Structural , Physical and Optical Properties of Borotellurite Glasses Incorporated with Silica from Rice Husk", J. Sci. Math. Lett. **6** (2018) 32.

[11] Umar et al., "Physical, structural and optical properties of erbium doped rice husk silicate borotellurite (Er-doped RHSBT) glasses", J. Non. Cryst. Solids **472** (2017) 31, doi: 10.1016/j.jnoncrysol.2017.07.013.

[12] Y. Azlina, M. N. Azlan, M. K. Halimah, S. A. Umar, R. El-mallawany, and G. Najmi, "Optical performance of neodymium nanoparticles doped tellurite glasses", Phys. B Phys. Condens. Matter **577** (2020) 411784, doi: 10.1016/j.physb.2019.411784.

[13] M. N. . Azlan, M. K. Halimah, S. S. Hajer, A. B. Suraini, Y. Azlina, and S. A. Umar, "Enhanced Optical Performance of Tellurite Glass Doped with Samarium Nanoparticle for Fiber Optics Application", Chalcogenide Lett. **16** (2019) 215, doi: 10.1016/j.jnoncrysol.2017.07.013.

[14] M. N. Azlan et al., "Linear and Nonlinear Optical Efficiency of Novel Neodymium Nanoparticles Doped Tellurite Glass for Advanced Laser Glass", Educ. JSMT **5** (2018) 47.

[15] S. A. Umar and G. G. Ibrahim, "Theoretical Elastic Moduli of TeO2 – B2O3 – SiO2 Glasses", Educ. JSMT **7** (2020) 18.

[16] B. Suresh et al., "Enhancement of orange emission of Co2+ ions with Bi3+ ions in lead silicate glasses", J. Lumin., **172** (2016) 47, doi: 10.1016/j.jlumin.2015.11.018.

[17] S. A. Umar et al., "Spectroscopic investigations of Er2O3 doped silica borotellurite glasses", Opt. Mater. (Amst). **114** (2021) 110987, doi: 10.1016/j.optmat.2021.110987.

[18] D. Bellucci, A. Sola, R. Salvatori, A. Anesi, L. Chiarini, and V. Cannillo, "Role of magnesium oxide and strontium oxide as modifiers in silicate-based bioactive glasses: Effects on thermal behaviour, mechanical properties and in-vitro bioactivity", Mater. Sci. Eng. C **72** (2017) 566, doi: 10.1016/j.msec.2016.11.110.

[19] S. A. Umar, M. K. Halimah, K. T. Chan, and A. A. Latif, "Polarizability, optical basicity and electric susceptibility of Er3 + doped silicate borotellurite glasses", J. Non. Cryst. Solids **471** (2017) 101, doi: 10.1016/j.jnoncrysol.2017.05.018.

[20] A. Makishima and J. D. Mackenzie, "Direct calculation of Young's modulus of glass", J. Non. Cryst. Solids **12** (1973) 35, doi: 10.1016/0022-3093(73)90053-7.

[21] A. Makishima and J. D. Mackenzie, "Calculation of bulk modulus, shear modulus and Poisson's ratio of glass", J. Non. Cryst. Solids **17** (1975) 147, doi: 10.1016/0022-3093(75)90047-2.

[22] J. Rocherulle, C. Ecolivet, M. Poulain, P. Verdier, and Y. Laurent, "Elastic moduli of oxynitride glasses. Extension of Makishima and Mackenzie's theory", J. Non. Cryst. Solids **108** (1989) 187, doi: 10.1016/0022-3093(89)90582-6.

[23] S. H. Alazoumi, H. A. A. Sidek, M. K. Halimah, K. A. Matori, M. H. M. Zaid, and A. A. Abdulbaset, "Synthesis and elastic properties of ternary ZnO-PbO-TeO2 glasses", Chalcogenide Lett. **14** (2017) 303.

[24] Y. B. Saddeek and L. A. El Latif, "Effect of TeO 2 on the elastic moduli of sodium borate glasses", Phys. B, **348** (2004) 475, doi: 10.1016/j.physb.2004.02.001.

[25] A. A. El-Moneim and A. Abd El-Moneim, "Bond compression bulk modulus and Poisson's ratio of the polycomponent silicate glasses", Mater. Chem. Phys. **70** (2001) 340, doi: 10.1016/S0254-0584(00)00519-8.

[26] R. Laopaiboon and C. Bootjomchai, "Physical properties and thermoluminescence of glasses designed for radiation dosimetry measurements", Mater. Des. **80** (2015) 20, doi: 10.1016/j.matdes.2015.05.002.

[27] Y. B. Saddeek, "Structural analysis of alkali borate glasses", Phys. B Condens. Matter **344** (2004) 163, doi: 10.1016/j.physb.2003.09.254.

[28] A. Hesham, M. Samier, H. Afifi, and S. Marzouk, "Ultrasonic velocity and elastic moduli of heavy metal tellurite glasses", Mater. Chem. Phys. **80** (2003) 517, doi: 10.1016/S0254-0584(03)00099-3.

[29] M. S. Gaafar, S. Y. Marzouk, H. A. Zayed, L. I. Soliman, and A. H. S. El-deen, "Structural studies and mechanical properties of some borate glasses doped with different alkali and cobalt oxides", Curr. Appl. Phys. **13** (2014) 152, doi: 10.1016/j.cap.2012.07.007.

[30] L. Hasnimulyati, M. K. Halimah, A. Zakaria, S. A. Halim, and M. Ishak, "A comparative study of the experimental and the theoretical elastic data of Tm3+doped zinc borotellurite glass", Mater. Chem. Phys. **192** (2017) 228, doi: 10.1016/j.matchemphys.2017.01.086.

[31] N. Elkhoshkhany, R. El-Mallawany, and E. Syala, "Mechanical and thermal properties of TeO2–Bi2O3–V2O5–Na2O–TiO2glass system", Ceram. Int. **42** (2016) 19218, doi: 10.1016/j.ceramint.2016.09.086.

[32] L.-G. G. Hwa, C. L. Lu, and L.-C. C. Liu, "Elastic moduli of calcium alumino-silicate glasses studied by Brillouin scattering", Mater. Res. Bull. **35** (2000) 1285, doi: 10.1016/S0025-5408(00)00317-2.

[33] K. A. Matori, M. I. Sayyed, H. A. A. Sidek, M. H. M. Zaid, and V. P. Singh, "Comprehensive study on physical, elastic and shielding properties of lead zinc phosphate glasses", J. Non. Cryst. Solids **457** (2017) 97, doi: 10.1016/j.jnoncrysol.2016.11.029.

[34] A. A. El-Moneim and A. Abd El-Moneim, "Correlation between acoustical and compositional parameters of borate and tellurite glasses", Mater. Chem. Phys. **135** (2012) 653, doi: 10.1016/j.matchemphys.2012.05.040.

[35] Y. B. Saddeek, "Structural and acoustical studies of lead sodium borate glasses", J. Alloys Compd. **467** (2009) 14, doi: 10.1016/j.jallcom.2007.11.126.

[36] M. S. Gaafar, M. A. M. Abdeen, and S. Y. Marzouk, "Structural investigation and simulation of acoustic properties of some tellurite glasses using artificial intelligence technique", J. Alloys Compd. **509** (2011) 3566, doi: 10.1016/j.jallcom.2010.12.064.

[37] B. P. Hamid-reza et al., "Ultrasonic and optical properties and emission of Er3+ / Yb3+ doped lead bismuth-germanate glass affected by Bi+ / Bi2+ ions", J. Lumin. **143** (2013) 526, doi: 10.1016/j.jlumin.2013.05.053.

[38] Y. B. Saddeek, "Ultrasonic study and physical properties of some borate glasses", Mater. Chem. Phys. **83** (2004) 222, doi: 10.1016/j.matchemphys.2003.09.051.

[39] M. M. K. Halimah et al., "Ultrasonic Study and Physical Properties of Borotellurite Glasses", Am. J. Appl. Sci. **2** (2005) 1541.

[40] R. El-Mallawany, M. I. Sayyed, and M. G. Dong, "Comparative shielding properties of some tellurite glasses: Part 2", J. Non. Cryst. Solids **474** (2017) 16, doi: 10.1016/j.jnoncrysol.2017.08.011.

[41] E. S. Yousef, A. El-Adawy, and N. El-KheshKhany, "Effect of rare earth (Pr2O3, Nd2O3, Sm2O3, Eu2O3, Gd2O3and Er2O3) on the acoustic properties of glass belonging to bismuth-borate system", Solid State Commun. **139** (2006) 108, doi: 10.1016/j.ssc.2006.05.022.

[42] W. Chinnamat, R. Laopaiboon, J. Laopaiboon, S. Pencharee, and C. Bootjomchai, "Influence of ionic radius modifying oxides on the elastic properties of glasses using ultrasonic techniques and FTIR spectroscopy", Phys. Chem. Glas. Eur. J. Glas. Sci. Technol. Part B **58** (2017) 207, doi: 10.13036/17533562.58.5.101.

[43] S. A. Umar et al., "Structural , elastic and thermo - physical properties of Er2O3 nanoparticles doped bio-silicate borotellurite glasses", SN Appl. Sci. **291** (2020) 1, doi: 10.1007/s42452-020-2112-x.

[44] R. A. Tafida et al., "Structural, optical and elastic properties of silver oxide incorporated zinc tellurite glass system doped with Sm3+ ions", Mater. Chem. Phys. **246** (2020) 122801, doi: 10.1016/j.matchemphys.2020.122801.